SPECTRAL RETRIEVAL OF LATENT HEATING PROFILES FROM TRMM PR DATA: COMPARISON OF LOOK-UP TABLES

Shoichi Shige[1,*], Yukari N. Takayabu[2], Wei-Kuo Tao[3] and Chung-Lin Shie[3,4]

[1]Department of Space Engineering, Osaka Prefecture University, Osaka, Japan
[2]Center for Climate System Research, University of Tokyo, Tokyo, Japan
[3]Laboratory for Atmospheres, NASA/Goddard Space Flight Center, Greenbelt, Maryland, U.S.A.
[4]Goddard Earth Sciences and Technology Center, University of Maryland, Baltimore County, Baltimore, Maryland, U.S.A.

1. INTRODUCTION

The Spectral Latent Heating (SLH) algorithm has been developed for the TRMM PR (Shige et al., 2004). Heating profile lookup tables for the three rain types; convective, shallow stratiform, and anvil rain (deep stratiform with a melting level) were produced with numerical simulations of tropical cloud systems in TOGA-COARE. For convective and shallow stratiform regions, the lookup table refers to the precipitation top height (PTH). For anvil region, on the other hand, the lookup table refers to the precipitation rate at the melting level instead of PTH.

It is necessary to examine the universality or regionality of the lookup table for global application of the SLH algorithm to TRMM PR data. If relationship between precipitation profiles and associated latent heating profiles change between regions, the lookup table would produce large error. In this study, we compare the lookup table from TOGA-COARE (western Pacific warm pool), GATE (eastern Atlantic) and SCSMEX (South China Sea) simulations to examine the universality or regionality of the lookup table.

2. APPROACH

Due to the scarcity of reliable validation data and difficulties associated with the collocation of validation data and satellite measurements, a consistency check of the SLH algorithm is performed, using CRM-simulated precipitation profiles as a proxy for the PR data. The algorithm-reconstructed heating profiles from CRM-simulated precipitation profiles are compared to CRM-simulated "true" heating profiles, which are computed directly from the model thermodynamic equation.

Here the 2-D version of the Goddard Cumulus Ensemble (GCE) model (Tao and Simpson, 1993) is used. Numerical simulations were conducted with the large-scale forcing data from TOGA-COARE (Ciesielski et al., 2003), GATE (Sui and Yanai, 1986), SCSMEX (Johnson and Ciesielski, 2002).

*Corresponding author address: Dr. Shoichi Shige, Department of Space Engineering, Osaka Prefecture University, 1-1 Gakuen-cho, Sakai, Osaka, 599-8531 Japan; e-mail: shige@aero.osakafu-u.ac.jp

3. RESULTS AND DISCUSSIONS

3.1. Consistency check

For a consistency check of the SLH algorithm, we reconstructed heating profiles averaged the GATE region for the 1–7 September 1974 period and the SCSMEX region for the 2–11 June 1998 period using the simulated parameters (i.e. PTH, convective/stratiform characteristics, P_s, P_m) as inputs. The lookup table produced from COARE simulations is used.

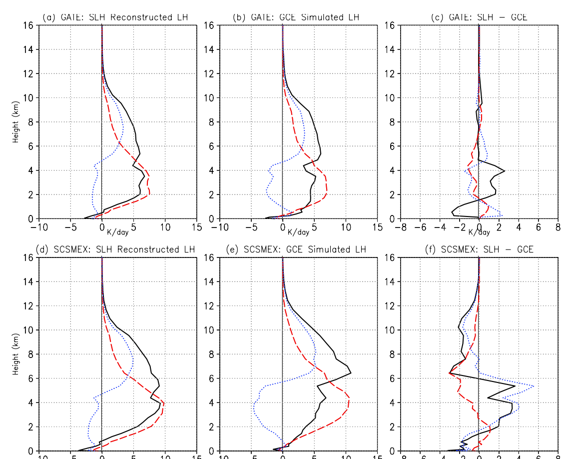

Figure 1: Profiles of latent heating rate in total (solid), convective (dashed), and stratiform (dotted) regions simulated from the GCE model for (a) GATE (Sep 1-7 1974) and (d) SCSMEX (Jun 2-11 1998). Reconstructed using the SLH algorithm with the COARE table for (b) GATE and (e) SCSMEX. Simulated minus reconstructed for (c) GATE and (f) SCSMEX.

The COARE table produces good agreement between SLH-algorithm reconstructed and GCE simulated heating profiles for GATE (Fig. 1a–c). On the other hand, the COARE table produces poorer agreement between SLH-algorithm reconstructed and GCE simulated heating profiles for SCSMEX than GATE (Fig. 1d–f). The top heaviness of reconstructed total heating profile using the COARE table is weaker than simulated one. There are two major reasons for the disagreement between reconstructed and GCE simulated heating profile. First, the reconstructed convective heating decrease more rapidly with height above the freezing level than the simulated one does. Second, the reconstructed cooling maximum in the stratiform region locates lower level than the simulated one.

3.2. Comparisons of lookup tables

Figure 2a–c show lookup tables for the convective region produced from COARE, GATE and SCSMEX simulations. The latent heating profiles are sorted referring to the precipitation top height (PTH) with a threshold of 0.3 mm h^{-1}. It should be noted that latent heating normalized by the convective rain fall is shown. The GATE table is similar to the COARE table. Both COARE and GATE convective cells have latent heating concentrated below the freezing level, indicating "oceanic" characteristics with enhanced liquid water processes (i.e. condensation). On the other hand, SCSMEX convective cells have stronger latent heating above the freezing level, indicating "continental" characteristics with significant ice processes (i.e., riming and/or depositional growth). These differences account for the disagreement between reconstructed and GCE simulated heating profile in convective regions.

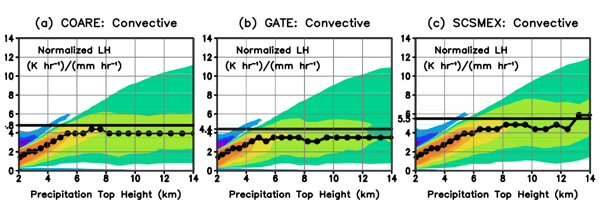

Figure 2: Lookup tables for the convective region produced from (a) COARE, (b) GATE, and (c) SCSMEX simulations. Horizontal lines indicate the 0 ^{o}C levels. Closed circles indicate heating maximum in convective tables.

Fig. 3d–f show lookup tables for the anvil (deep stratiform with a melting level) regions produced from COARE, GATE and SCSMEX simulations. Considering the insensitivity of PR to the small ice-phase hydrometeors, the precipitation rate at the melting level is selected instead of PTH as a parameter for the lookup table for the anvil regions in the SLH algorithm. In the COARE and GATE tables, the maximum cooling locates in z = 1 km to z = 2 km. On the other hand, in the SCSMEX table, the maximum in cooling locates in z = 3 km to z = 4 km, much higher than the COARE and GATE tables. These differences explain the disagreement between reconstructed and GCE simulated heating profile in stratiform regions.

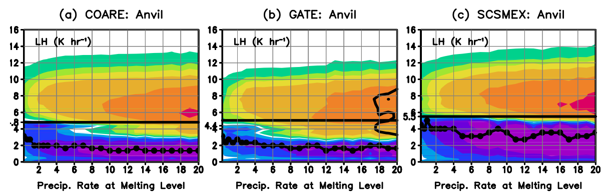

Figure 3: Lookup tables for the convective region produced from (a) COARE, (b) GATE, and (c) SCSMEX simulations. Horizontal lines indicate the 0 ^{o}C levels. Closed circles indicate heating maximum in convective tables.

Figure 4 shows profiles of convective heating, stratiform heating and rear inflow (RI) for the COARE December 24 1992 and the SCSMEX June 5 1998 cases. Both are typical squall lines for each region. The depth of stratiform cooling is consistent with that of RI that brings dry air into the system. Stratiform cooling and RI are shallow in the COARE case, while those are deep in the SCSMEX case. These differences explain those between COARE and SCSMEX lookup tables for anvil rain.

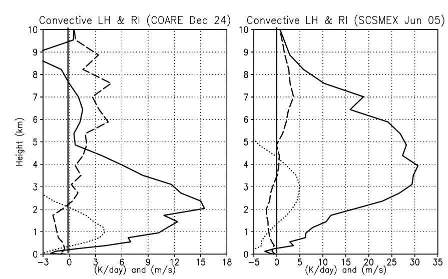

Figure 4: Profiles of convective heating (solid), stratiform heating (dashed), and rear inflow (RI: dotted) in COARE December 24 and SCSMEX June 5.

3.3. Algorithm improvement for convective heating

To distinguish convective characteristics between the "oceanic" and "continental" regimes, heating amplitude below and above the freezing (melting) level should be determined separately. The vertically-integrated heating, $Q = (LH, Q_{1R})$, from the melting level z_m to the tropopause z_t may be related to the precipitation rate at the melting level P_m by

$$\int_{z_m}^{z_t} \rho Q(z) \triangle z = \frac{L_v}{C_p} P_m \cdot (1 + f_u) \tag{1}$$

where f_u is the fraction of the precipitation rate at the melting level, P_m, generated in and carried over from the upper layers of the convective region. The P_m is used as an additional index for the table for convective rain. The GCE-simulated precipitation profiles with 0.3 mm hr^{-1} precipitation top threshold and corresponding heating profiles are accumulated and averaged for each PTH and each P_m range with model grid intervals. The ranges of the P_m are summarized in Table 1. For construction of lookup tables, the GCE-simulated outputs from the four subperiods of 9-day durations (10-18 December 1992, 27 December 1992 - 4 January 1993, 9-17 February 1993, and 18-26 February 1993) are used as well as Shige et al. (2004).

Range of P_m					
	0-5	5-10	10-15	15-20	25-30
	30-35	30-35	35-40	40-50	50-60
	70-80	80-90	90-100	100-	

Table 1: Range of P_m (mm hr^{-1})

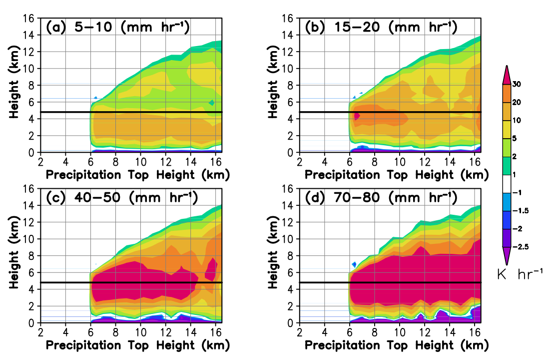

Figure 5: Convective lookup tables for the four ranges of the P_m. Horizontal lines indicate the 0 ^{o}C levels.

The tables for the four ranges of the P_m are shown in (Fig. 5). In the table for the small P_m range (Fig. 5a), the level of LH peak does not change with PTH, and it remains below the melting level. This indicates that liquid water processes dominate. The level of LH peak for a given PTH shifts upward and the heating amplitude above the melting level increases with P_m (Fig. 5b-c). This indicates that ice processes enhance with P_m. Thus, it is appropriate use the PTH as an additional index for tables for convective rain. For all range pf P_m, heating top height increases with PTH, so that the PTH is an appropriate index for determination of heating top height.

For convective regions, a heating profile corresponding to the PTH and P_m is selected in the convective heating profile (Fig. 6). The amplitude below the melting level is determined by

$$Q(z)_{low} = \frac{\widetilde{Q}_{low}(z)}{\widetilde{P}_s} \cdot P_s, \tag{2}$$

while that above the melting level is determined by

$$Q(z)_{high} = \frac{\widetilde{Q}_{high}(z)}{\widetilde{P}_m} \cdot P_m. \tag{3}$$

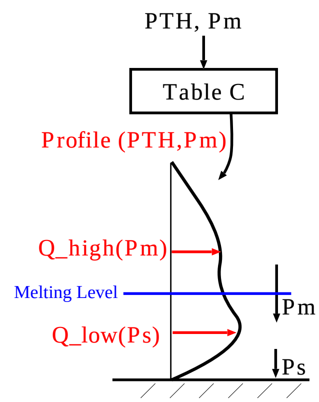

Figure 6: Diagram showing the procedure for deriving convective latent heating profiles using the spectral latent heating (SLH) algorithm. See the text for details.

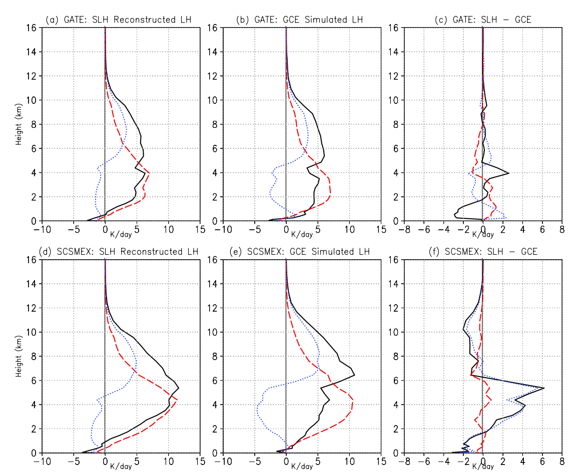

Figure 7: Same as Fig. 7, but for reconstructed using the revised SLH algorithm.

For an evaluation of the above retrieval procedure for convective rain, we reconstructed heating profiles for the GATE and SCSMEX simulations. Figure 7 shows that the revised retrieval procedure produces much better agreement between SLH reconstructed and GCE simulated convective heating profiles for SCSMEX than the original one (Fig. 1). The revised algorithm-reconstructed heating above the melting level is stronger than the original algorithm-reconstructed one and is good agreement with GCE simulated one. This is because heating amplitude associated with liquid water processes below and that associated with ice processes above the freezing (melting) level are determined separately.

4. SUMMARY AND FUTURE WORK

In this study, the universality or regionality of the lookup table produced from COARE simulations (Shige et al., 2004) was examined for global application of the SLH algorithm to TRMM PR data. We reconstructed heating profiles from CRM-simulated parameters (i.e. PTH, precipitation rate at the melting level, rain rate and type) with the TOGA-COARE table and compared them to CRM-simulated " true " heating profiles, which were computed directly the model thermodynamic equation. The GATE and SCSMEX periods were used for consistency check. The consistency check showed that TOGA-COARE table produced poorer agreement for SCSMEX than GATE due to the two reasons. First, convection has " oceanic "characteristics with enhanced liquid water processes for the TOGA-COARE and GATE cases, while it has " continental " characteristics with significant ice processes for the SCSMEX case. Second, there are differences in the stratiform cooling shapes, due to differences in the location of the rear inflow.

To distinguish convective characteristics between the "oceanic" and "continental" regimes, we use the precipitation rate at the melting level (P_m) as an additional index for the lookup table for convective rain. For a consistency check of the revised SLH algorithm, we reconstructed heating profiles for the GATE and SCSMEX periods with the revised convective lookup tables produced the TOGA-COARE simulations. The revised SLH algorithm produces much better agreement between reconstructed and GCE simulated convective heating profiles for SCSMEX than the original one. This is because heating amplitude below and above the freezing (melting) level are determined separately.

Still, there are notable disagreement between SLH reconstructed and GCE simulated lower-level cooling in the stratiform regions for SCSMEX (Fig. 7). Melting and evaporative cooling should be related to precipitation profiles. Hydrometeors heating algorithm, which estimates latent heating from hydrometer profiles, has shown that the derived cooling are good agreement with those calculated explicitly from the GCE model (Tao et al., 1990). It may be necessary to use more information about the precipitation profiles for algorithm improvement for stratiform rain.

Acknowledgement This study is supported by the JAXA/EORC Tropical Measuring Mission (TRMM) project. Comments by Drs. T. Iguchi and H. Masunaga are appreciated. W.-K. Tao and C.-K. Shie are mainly supported by the NASA headquarters Atmospheric Dynamics and Thermodynamics Program and the NASA TRMM. They thank Dr. R. Kakar at NASA headquarters for his support.

REFERENCES

Ciesielski, P. E., R. H. Johnson, P. T. Haertel, and J. Wang: 2003, Corrected TOGA COARE sounding humidity data: Impact on diagnosed properties of convection and climate over the warm pool. *J. Climate*, **16**, 2370–2384.

Johnson, R. H. and P. E. Ciesielski: 2002, Characteristics of the 1998 summer monsoon onset over the northern South China Sea. *J. Meteor. Soc. Japan*, **80**, 561–578.

Shige, S., Y. N. Takayabu, W.-K. Tao, and D. E. Johnson: 2004, Spectral retrieval of latent heating profiles from TRMM PR data. part I: Development of a model-based algorithm. *J. Appl. Meteor.*, **43**, 1095–1113.

Sui, C. H. and M. Yanai: 1986, Cumulus ensemble effects on the large-scale vorticity and momentum fileds of GATE. Part I: Observational evidence. *J. Atmos. Sci.*, **43**, 1618–1642.

Tao, W.-K. and J. Simpson: 1993, Goddard cumulus ensemble model. Part I: Model description. *Terr. Atmos. Oceanic Sci.*, **4**, 35–72.

Tao, W.-K., J. Simpson, S. Lang, M. McCumber, R. Adler, and R. Penc: 1990, An algorithm to estimate the heating budget from vertical hydrometer profiles. *J. Appl. Meteor.*, **29**, 1232–1244.